DNA Cross-Linking with Metallointercalator−Peptide Conjugates†

Kimberly D. Copeland, Alexis M. K. Lueras, Eric D. A. Stemp,*,‡ and Jacqueline K. Barton*

Division of Chemistry and Chemical Engineering, California Institute of Technology, Pasadena, California 91125

Received June 7, 2002; Revised Manuscript Received August 21, 2002

ABSTRACT: Short peptides have been tethered to a DNA−intercalating ruthenium complex to create a photoactivated cross-linking reagent. The ruthenium complex, $[Ru(phen)(bpy')(dppz)]^{2+}$ (phen = 1,10-phenanthroline, bpy′ = 4-(butyric acid)-4′-methyl-2,2′-bipyridine, and dppz = dipyridophenazine), delivers the peptide to DNA and initiates the cross-linking reaction by oxidizing DNA upon irradiation in the presence of an oxidative quencher. The tethered peptide, only five to six residues in length, forms cross-links with the oxidized site in DNA. Cross-linking was detected and studied by gel electrophoresis and through spectroscopic measurements. The ruthenium−peptide complex is luminescent when bound to DNA, and the binding constants for several intercalator−peptide conjugates were determined by luminescence titration. The composition of the peptide affects both binding affinity and the extent of cross-linking. The greatest amounts of cross-linking were observed with tethered peptides that contained positively charged residues, either lysine or arginine. To test the impact of individual residues on cross-linking, the central residue in a 5-mer peptide was substituted with seven different amino acids. Though mutation of this position had only a small effect on the extent of cross-linking, it was discovered that peptides containing Trp or Tyr gave a distinctive pattern of products in gels. In experiments using the untethered peptide and ruthenium complex, it was determined that delivery of the peptide by the ruthenium intercalator is not essential for cross-linking; peptide attachment to the metal complex can constrain cross-linking. Importantly, the cross-linking adducts produced with ruthenium−peptide conjugates are luminescent and thus provide a luminescent cross-linking probe for DNA.

Oxidative damage to DNA has been implicated as a factor in aging and in diseases, including cancers, neurodegenerative disorders, and chronic inflammatory diseases (*1*−*4*). Oxidative damage can lead to a variety of DNA lesions, and one important but poorly characterized lesion is the DNA−protein cross-link (*5*−*7*). Many endogenous and environmental agents can produce covalents links between DNA and protein (*5*, *6*), and these cross-links are now recognized as a biomarker for aging and disease (*8*). The cell likely employs a number of strategies for the removal of these structurally diverse and bulky lesions, and recent studies have suggested a role for nucleotide excision repair proteins and ubiquitin-dependent proteases (*5*, *9*).

DNA−protein cross-links have been demonstrated with transition metal complexes, for example, with complexes of Ni(II), Cr(VI), and Fe(II), and with (1,10-phenanthroline)-Cu(II) (*10*−*13*). In a recent study, specific cross-linking between the MutY protein and a duplex containing 8-oxoG[1] was initiated by the one-electron oxidant Na_2IrCl_6 (*14*). A number of chemotherapeutic reagents, including cisplatin, neocarcinostatin, and iron(III) bleomycin, have also been shown to form DNA−protein cross-links (*7*, *13*, *15*, *16*). The mutagenic effects of aldehydes have been attributed primarily to DNA−protein cross-linking (*17*−*19*). Finally, cross-linking can be induced by exposure to UV light, visible light with $^1O_2$ photosensitizers, or ionizing radiation (*20*−*25*).

Although a variety of reagents and methods have been demonstrated to initiate DNA−protein cross-linking, the molecular details of cross-linking and the exact nature of the cross-linking lesions are still under investigation. Simple model systems have been very valuable in providing insight into the molecular mechanisms of cross-linking. For example, using a well-characterized model system, Morin and Cadet have demonstrated that 1-electron-oxidized 2′-deoxyguanosine reacts with both hydroxyl- and amino-based nucleophiles to form covalent adducts (*26*−*28*). The cross-linking products were identified, and it was determined that cross-linking occurred at the C8 position of guanine. Here we describe the development of a metallointercalator−peptide conjugate, a new model system, for the study of DNA−protein cross-linking.

A family of octahedral metallointercalators that bind to and react with DNA has been prepared in our laboratory (*29*). The metallointercalators are substitutionally inert complexes of rhodium and ruthenium, and they boast aromatic heterocyclic ligands. The planar aromatic ligands

† This work was supported by the NIH (GM33309). The NIH also provided an NRSA predoctoral fellowship (K.D.C.), and the MURF program at Caltech provided a summer fellowship (A.M. K.L.).

* To whom correspondence should be addressed. E-mail: jkbarton@its.caltech.edu and estemp@msmc.la.edu.

‡ Present address: Department of Physical Sciences, Mount St. Mary's College, Los Angeles, CA 90049.

[1] Abbreviations: phen, 1,10-phenanthroline; bpy′, 4-(butyric acid)-4′-methyl-2,2′-bipyridine; dppz, dipyrido[3,2-*a*:2′,3′-*c*]phenazine; 8-oxo-G, 7,8-dihydro-8-oxoguanine; FAPy-G, 2,6-diamino-5-formamido-4-hydroxypyrimidine; DBU, 1,8-diazabicyclo[5.4.0]undec-7-ene; DMF, *N*,*N*-dimethylformamide; TFA, trifluoroacetic acid; TIS, triisopropylsilane; PyBOP, benzotriazol-1-yloxytris(pyrrolidino)phosphonium hexafluorophosphate.

10.1021/bi020407b CCC: $22.00
Published on Web 09/26/2002

Scheme 1: Diagram of the Flash−Quench Cycle

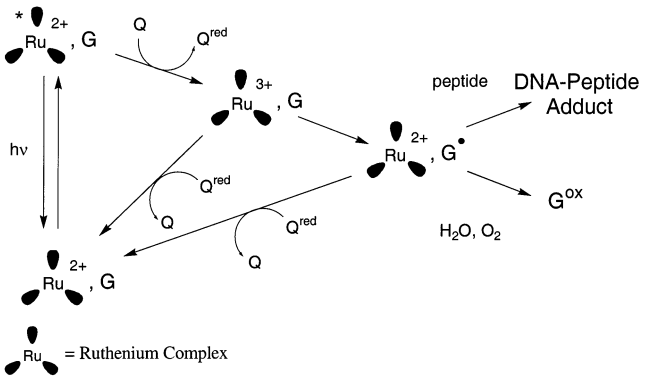

G = guanine site in DNA, Q = oxidative quencher, Q^{red} = reduced quencher, $G^{\bullet}$ = guanine radical, G^{ox} = permanent guanine lesions.

insert deeply between the DNA base pairs, without causing significant disruptions in DNA conformation (*30*). The intercalating and ancillary ligands of these complexes have been varied systematically to achieve site specificity and reactivity. As a result, the metallointercalators provide useful probes of DNA structure and DNA-mediated electron transfer (*31*, *32*).

Short peptides can be tethered to metallointercalators to give conjugates with novel recognition or reactive properties. Through the attachment of a 13-mer recognition helix from a DNA binding protein, we transformed a sequence-neutral rhodium complex into an intercalator that preferentially targets the sequence 5′-TCA-3′ (*33*). By attaching metal-binding peptides to a rhodium intercalator, we were able to promote hydrolysis or oxidative cleavage of the DNA backbone (*34*, *35*). These studies, as well as studies from other laboratories (*36*, *37*), demonstrate that DNA intercalators can be harnessed for the delivery of peptides to DNA.

Dipyridophenazine complexes of ruthenium, such as $[Ru(bpy)_2dppz]^{2+}$ and $[Ru(phen)_2dppz]^{2+}$, are particularly useful probes for DNA. These complexes have rich spectroscopic properties and show dramatic changes in luminescence on DNA binding. Indeed, they have been dubbed molecular "light switches" for DNA; in aqueous solutions the complexes show no detectable photoluminescence, but on the addition of DNA, intense emission centered around 610 nm is observed (*38*, *39*). Intercalation of the dppz ligand into DNA protects the phenazine nitrogen atoms from water and thus blocks solvent quenching of the luminescence of the excited state (*38*, *40*). Also, the redox properties of these dppz complexes of ruthenium have facilitated the study of charge transport through DNA (*41*, *42*). In particular, the dipyridophenazine−Ru(III) complex, generated in situ using the flash−quench technique, serves as a potent DNA oxidant and yields long-range oxidative damage to DNA.

The flash−quench technique, originally developed for the study of protein electron transfer (*43*), has been successfully adapted for studies with DNA (*41*, *42*, *44*, *45*). In a flash−quench experiment (Scheme 1), a photosensitive DNA intercalator, such as $[Ru(phen)_2dppz]^{2+}$ or $[Ru(phen)(bpy')(dppz)]^{2+}$, is excited by irradiation with visible light. The excited-state species surrenders an electron to an oxidative quencher and is converted into a strong oxidant (1.6 V). The oxidized intercalator can then undergo back-electron transfer with the reduced quencher or can steal an electron from a guanine site in DNA.

Of all the DNA bases, guanine has the lowest oxidation potential (1.3 V) (*46*) and is the most vulnerable to oxidative damage, particularly when two or three guanines are clustered together on a DNA strand (*47*−*49*). Using the $[Ru(phen)_2dppz]^{2+}$ intercalator and $[Ru(NH_3)_6]^{3+}$ as quencher in a flash−quench experiment, the neutral guanine radical has been seen in poly(dG-dC) by transient absorption spectroscopy (*45*). Because DNA is an effective medium for charge transport, the guanine radical is very mobile in DNA. Indeed, guanine damage has been observed over distances as great as 200 Å from a tethered oxidant (*50*−*52*). Permanent guanine damage results when the guanine radical reacts with oxygen or with water to form products such as 8-oxo-G, Fapy-G, oxazolone, or imidazolone (*53*−*55*).

The flash−quench chemistry of $[Ru(phen)_2dppz]^{2+}$ has also been applied in exploring electron transfer between DNA and proteins. Can proteins sense oxidative damage to DNA or participate in electron-transfer reactions with DNA? To probe these questions, we used free $[Ru(phen)_2dppz]^{2+}$ or a DNA−tethered $[Ru(phen)(bpy')(dppz)]^{2+}$ complex and the tripeptides Lys-Tyr-Lys or Lys-Trp-Lys (*56*, *57*). These peptides bind with modest affinity to DNA; the positively charged Lys residues associate with the polyanionic backbone, and the aromatic residue can intercalate. For example, a Lys-Trp-Lys-Gly peptide has a dissociation constant of 5.9×10^{-4} M for *Escherichia coli* DNA and binds with slightly higher affinity to AT alternating sequences or at abasic sites (*58*, *59*). Also, the aromatic residues are thermodynamically vulnerable to oxidation by the guanine radical, since the oxidation potentials of Tyr, Trp, and the guanine radical are 0.9, 1.0, and 1.3 V (*45*, *57*). With this system, we demonstrated that electron transfer occurs from peptides to DNA. By transient absorption spectroscopy, both the Trp and Tyr radical were detected (*56*, *57*). The guanine radical was found to be a key intermediate in the peptide-to-DNA electron transfer; indeed, the rise of the Tyr radical signal and the disappearance of the guanine radical signal occurred with the same kinetics, and no Trp or Tyr radical was observed in studies with a poly(dA·dT) substrate. Importantly, we found that the peptide radicals produced by the flash−quench reaction could lead to DNA−peptide cross-links. Cross-linking adducts were detected for the Lys-Tyr-Lys peptide but not for the Lys-Trp-Lys peptide.

If proteins are included in the flash−quench reaction, the guanine radical also can react to form DNA−protein cross-links. Recently, Nguyen et al. introduced this strategy for forming cross-links (*6*). By exploiting the flash−quench chemistry of $[Ru(phen)_2dppz]^{2+}$, they were able to produce covalent adducts between DNA and histone protein, presumably through nucleophilic attack by amino acid residues at the guanine radical. The extent of cross-linking was found to depend on the quencher, and in experiments with $[Co(NH_3)_5Cl]^{2+}$, methyl viologen, and $[Ru(NH_3)_6]^{3+}$ they found that the cobalt quencher, a sacrificial quencher that decomposes upon reduction, produced the highest levels of cross-linking (*6*). Building on our work with tripeptides and the foundation laid by Nguyen et al., we now are using the flash−quench technique to create DNA−peptide adducts.

By attaching very short peptides to a ruthenium intercalator, we have created a model system for the study of DNA−protein cross-linking (Figure 1). The ruthenium intercalator, $[Ru(phen)(bpy')(dppz)]^{2+}$, serves three important

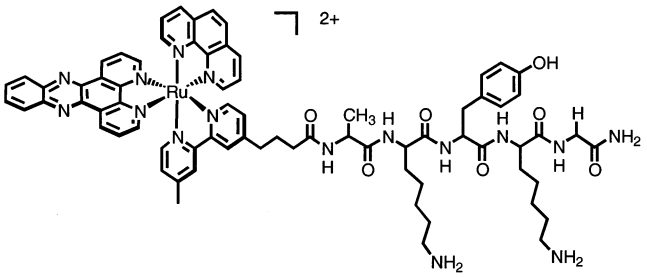

FIGURE 1: The metallointercalator−peptide conjugate [Ru(phen)(bpy′-AKYKG)(dppz)]$^{2+}$. The ruthenium intercalator provides binding affinity and participates in a flash−quench reaction that oxidizes DNA. The tethered peptide forms covalent cross-links at the oxidized site in DNA.

roles: (i) through the flash−quench reaction it oxidizes DNA and initiates cross-linking, (ii) it provides binding affinity for peptides that would not otherwise bind to DNA, and (iii) it serves as a luminescent tag. The peptide provides a variety of functional groups that can react with the oxidized DNA to produce cross-links and can be conveniently tuned to explore the potential of different peptide compositions for cross-linking.

MATERIALS AND METHODS

Synthesis of Ligands and Metal Complexes. The ligands and metal complexes were synthesized as described in the literature (*60*−*65*).

Preparation of Peptides. Peptides were synthesized on solid support by the Beckman Institute Biopolymer Synthesis Facility at Caltech using an ABI 433 peptide synthesizer and N-Fmoc-l-amino acids and were supplied on the resin. All peptides were prepared with a carboxamide at the C-terminus. The N-terminal protecting group was manually removed with a 2% solution of 1,8-diazabicyclo[5.4.0]undec-7-ene in DMF, and the peptides were cleaved from the resin and deprotected with a cocktail of trifluoroacetic acid (TFA), water, and triisopropylsilane (TIS). The peptides were precipitated by filtration into ice-cold *tert*-butyl methyl ether, redissolved in 5% acetic acid, and lyophilized. Next they were purified by HPLC on a semipreparative Vyadac C18 reversed-phase column using the following solvents: A, water (0.1% TFA), and B, 70:30 water−acetonitrile (0.1% TFA). The percentage of solvent B was held at 10% for 5 min and was then increased to 100% over 35 min. Chromatograms were monitored at 220 and 260 nm, and the peptides eluted between 8 and 20 min. Peptides were quantitated by absorbance measurements, using $\epsilon_{280} = 1280$ M^{-1} cm^{-1} for tyrosine containing peptides, $\epsilon_{280} = 5690$ M^{-1} cm^{-1} for tryptophan-containing peptides, and $\epsilon_{205} = 13000$ M^{-1} cm^{-1} for peptides without aromatic residues (*66*).

Preparation of Ruthenium−Peptide Conjugates. Again, resin-bound peptides were received from the Beckman Institute Biopolymer Synthesis Facility, and the N-terminal protecting group was removed with DBU. The resin-bound peptides were combined with racemic [Ru(phen)(bpy′)(dppz)]$^{2+}$ (1 equiv), PyBOP (3 equiv), and diisopropylethylamine (6 equiv) in DMF and stirred at ambient temperature overnight. As with the free peptides, the conjugates were cleaved from the resin and deprotected with the TFA cocktail. The intercalator−peptide conjugates were HPLC purified on a semipreparative Vyadac C18 reversed-phase column using a water (0.1% TFA)−acetonitrile (0.1% TFA) gradient and a flow rate of 4 mL/min. The percentage of acetonitrile was held at 15% for 5 min and then increased from 15% to 40% over 20 min. Chromatograms were monitored at 260 and 440 nm, and the desired material eluted between 20 and 25 min. After lyophilization, the intercalator−peptide conjugates were obtained as fluffy orange solids.

Characterization of Ruthenium−Peptide Conjugates. MALDI mass spectrometry was used to verify the identity of the purified chimeras. The spectral characteristics of intercalator−peptide conjugates by UV−visible spectroscopy and NMR have been found generally to be the sum of those of the intercalator and peptide separately. The absorption of [Ru(phen)(bpy′)(dppz)]$^{3+}$ in the visible region ($\epsilon = 19000$ M^{-1} cm^{-1} at 440 nm) provides a convenient handle for quantification. The fractions isolated by HPLC for the Ru−KYK conjugate were analyzed by circular dichroism using an Aviv (62A DS) instrument. Samples of Ru−KYK (5 μM) were prepared in a sodium borate buffer (25 mM, pH 7), and spectra were obtained by scanning from 600 to 200 nm.

Binding Constant Determination. The [Ru(phen)(bpy′)(dppz)]$^{2+}$ complex is luminescent in the presence of DNA, and binding constants were determined for several ruthenium−peptide conjugates by luminescence titration. A dilute solution of the ruthenium−peptide conjugate (0.5 μM) was prepared and buffered with sodium phosphate (10 mM, pH 7). High sodium chloride concentrations (100 mM) were needed to drop the affinity of the conjugates into a measurable range. The ruthenium−peptide solution was titrated with solutions of calf thymus DNA (Pharmacia, dialyzed with buffer and quantitated by absorbance at 260 nm). To avoid dilution of the conjugate sample, the DNA solutions were prepared with a matching concentration of ruthenium−peptide. After each addition of DNA, the sample was excited at 442 nm, and the emission spectrum was obtained using an ISS K2 fluorometer. The area under the luminescence peak was determined and plotted against the log of DNA base pair concentration. The final luminescence value (L_f), the luminescence observed for fully bound ruthenium complex, was determined from a sigmoidal fit of this plot, and an initial luminescence value (L_i) was established from the spectrum obtained before the first addition of DNA. The fraction of bound ruthenium complex for each luminescence measurement (L) was determined using the expression:

$$\text{bound Ru/total Ru} = (L - L_i)/(L_f - L_i)$$

Using this fraction, the concentrations of bound and free ruthenium complex were determined for each DNA concentration, and a Scatchard plot was prepared by plotting R/C_{free} vs R (where R = concentration of bound ruthenium/concentration of DNA base pairs and C_{free} = concentration of free ruthenium) (*67*, *68*). The binding constant for an average binding site in the DNA substrate was obtained from the *y*-intercept of this plot, and the number of ruthenium complexes bound per base pair was obtained from the *x*-intercept.

Flash−Quench Cross-Linking with Ru−Peptides and Oligonucleotides. The strands of a 20-mer DNA duplex with one GG site (5′-TCA GAG TCT GGC TCG CAC TC-3′ and complement) and a 40-mer DNA duplex with four GG sites (5′-CGT GTA TTA CGG ACT ACG TAG GCT AGC

CAG CGT GGA ACG C-3′ and complement) were prepared using an ABI 392 DNA synthesizer, purified by HPLC, and annealed by slow cooling from 90 °C. In a typical flash−quench cross-linking reaction, the duplex (5 μM) was combined with conjugate (20 μM) and $[Co(NH_3)_5Cl]Cl_2$ quencher (200 μM) in a buffer containing sodium phosphate (10 mM, pH 7) and sodium chloride (20 mM). The total volume of each reaction was 20 μL. The quencher and ruthenium complex were added in the dark, and the sample was allowed to equilibrate for 10−20 min. Next the samples were irradiated at 442 nm for 1−30 min using a 1000 W Hg/Xe lamp equipped with a monochromator (power = 5−10 mW) or a He/Cd laser (power = 10−15 mW). A light control sample containing only duplex and a quencher control sample containing duplex and quencher were also irradiated. A dark control sample containing duplex, quencher, and ruthenium conjugate was not irradiated. After irradiations were completed, the samples were extracted with 1 volume of 1:1 phenol−chloroform and then with 1 volume of chloroform to remove noncovalent ruthenium−peptide from the samples.

Analysis of Cross-Linking by Gel Electrophoresis. For gel experiments, one strand of the DNA duplex was radiolabeled by incubation with [γ-^{32}P]ATP and polynucleotide kinase. The labeled strand was purified on a 10% polyacrylamide gel, excised and recovered from the gel by the crush and soak method (*69*), and desalted with BioSpin columns (Bio-Rad). The labeled strand was included in an annealing reaction with unlabeled strands. After the flash−quench reaction and extraction procedure, some samples were treated with 10% aqueous piperidine for 30 min at 90 °C to promote strand scission. All samples were dried and redissolved in denaturing (formamide, bromophenol blue, and xylene cyanol) or nondenaturing (glycerol and marker dyes) loading buffer. The samples were analyzed on 15% or 20% denaturing gels (2000 V, 2 h) or on 10% or 15% native gels (150 V, 3 h). The native gels were dried under vacuum in a gel dryer for 90 min at 80 °C. The gels were exposed to phosphor screens and visualized using a Phosphorimager. Using the ImageQuant program, the extent of cross-linking for a sample was estimated by integrating the counts above the parent band (corrected for background) and dividing by the counts in the entire lane (corrected for background).

Analysis of Cross-Linking by Absorbance Measurements. For absorbance experiments, ruthenium−peptide (20 μM), duplex (5 μM), quencher (200 μM), and buffer were combined to give a total reaction volume of 200 μL. Prior to the addition of the $[Co(NH_3)_5Cl]Cl_2$ quencher, a UV−vis spectrum was obtained for each sample using a Beckman DU 7400 spectrophotometer, and the absorbance at 440 nm was noted. After addition of the quencher, the samples were irradiated for 3 min at 442 nm with a He/Cd laser. The samples were mixed once during the irradiation by pipetting. After irradiation the samples were extracted, precipitated by the addition of ethanol, dried on the benchtop, and then redissolved in 1:1 water−acetonitrile. A second spectrum was obtained, and the fraction of cross-linked ruthenium−peptide conjugate was estimated from the ratio of absorbance at 440 nm before and after irradiation.

Characterization of Cross-Linked Material by Spectroscopy and Mass Spectrometry. To further characterize the cross-linking adducts, two identical samples containing ruthenium−peptide conjugate, quencher, and 20-mer duplex were prepared. One was irradiated at 442 nm, and one was kept in the dark. Both samples were extracted to remove noncovalent ruthenium complex from the sample and then were precipitated by the addition of ethanol. The material was redissolved in 1:1 water−acetonitrile, and absorption and luminescence spectra were obtained for each sample using a Beckman DU 7400 spectrophotometer and an ISS K2 fluorometer. In addition, several cross-linking samples were analyzed with an Applied Biosystems Voyager DE Pro MALDI TOF mass spectrometer. A saturated solution of 2,4,6-trihydroxyacetophenone was used for the laser desorption/ionization matrix (*70*).

Table 1: Ruthenium−Peptide Conjugates

abbreviation	conjugate[a]
Lys-Lys framework	
Ru−KAK	Ru−Ala-Lys-Ala-Lys-Gly-$CONH_2$
Ru−KEK	Ru−Ala-Lys-Ala-Lys-Gly-$CONH_2$
Ru−KHK	Ru−Ala-Lys-His-Lys-Gly-$CONH_2$
Ru−KKK	Ru−Ala-Lys-Lys-Lys-Gly-$CONH_2$
Ru−KSK	Ru−Ala-Lys-Ser-Lys-Gly-$CONH_2$
Ru−KWK	Ru−Ala-Lys-Trp-Lys-Gly-$CONH_2$
Ru−KYK	Ru−Ala-Lys-Tyr-Lys-Gly-$CONH_2$
Arg-Arg framework	
Ru−RYR	Ru−Ala-Arg-Tyr-Arg-Gly-$CONH_2$
6-mer peptide	
Ru−KYK-6	Ru−Gly-Ala-Lys-Tyr-Lys-Gly-$CONH_2$
Gly-Ala framework	
Ru−GAA	Ru−Ala-Gly-Ala-Ala-Gly-$CONH_2$
Ru−GKA	Ru−Ala-Gly-Lys-Ala-Gly-$CONH_2$
Ru−GYA	Ru−Ala-Gly-Tyr-Ala-Gly-$CONH_2$

[a] Ru = $[Ru(phen)(bpy')(dppz)]^{2+}$.

RESULTS

Preparation of Ruthenium−Peptide Conjugates. Using standard solid-phase peptide coupling strategies, short peptides have been coupled to the $[Ru(phen)(bpy')(dppz)]^{2+}$ complex to create a family of intercalator−peptide chimeras (Figure 1, Table 1). Although the dppz ligand can decompose in strong acid, it was found to be stable during peptide deprotection and cleavage, despite a 3 h treatment with TFA. The conjugates were synthesized cleanly and with modest overall yields (5−20%). The identity of the chimera was confirmed by mass spectrometry. Preparation of the Ru−AKCKG was attempted, but HPLC analysis of the crude material showed a large number of side products, and studies with this conjugate were abandoned.

The $[Ru(phen)(bpy')(dppz)]^{2+}$ complex has four different isomers (Figure 2). The arrangement of ligands around the metal center can be Δ or Λ, and the position of the carboxylate linker and peptide arm can be "axial" or "equatorial" to the dppz ligand. Two of these isomers were easily separated by standard HPLC, and for some conjugates the first well-resolved peak was split into two peaks. The HPLC chromatogram at 440 nm for the purification of the Ru−KYK conjugate is presented in Figure 2. For this conjugate the three HPLC peaks were separately collected. All three products were found by MALDI mass spectrometry to be identical and to have the expected mass of the Ru−KYK conjugate.

To further probe the identity of the separated products, the material from peaks 1, 2, and 3 was analyzed by circular

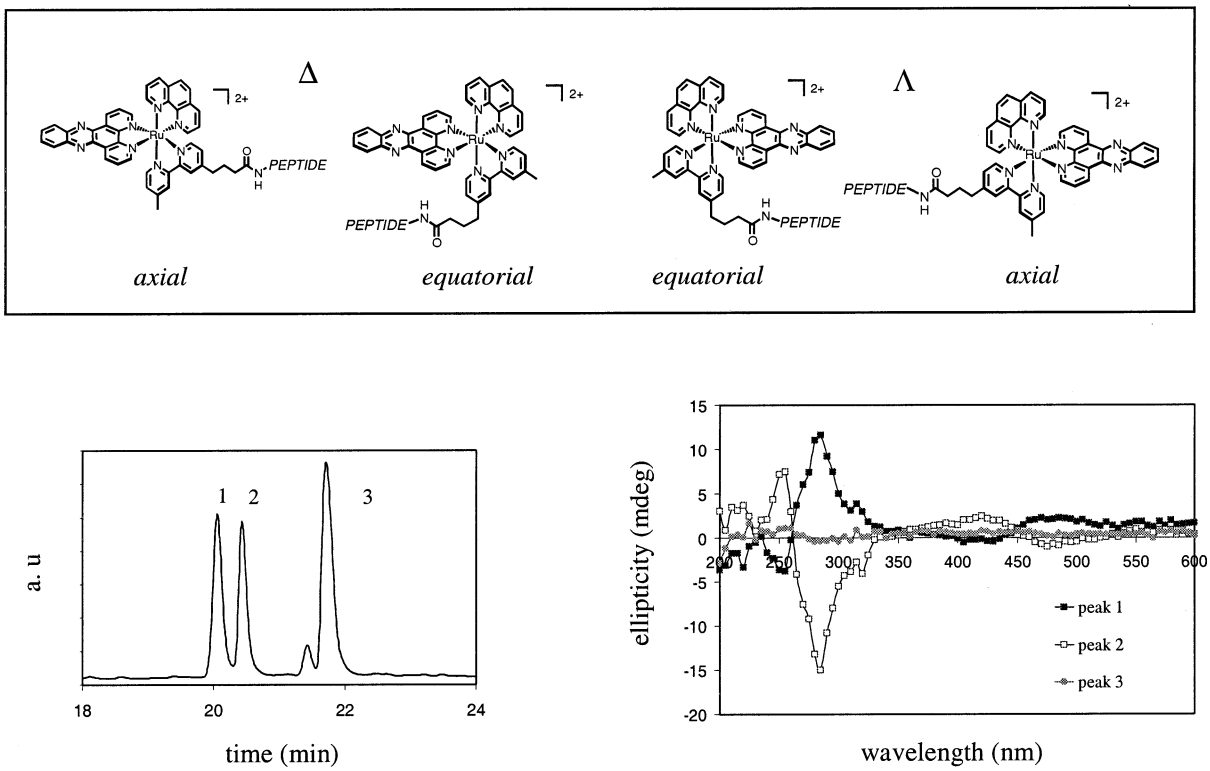

FIGURE 2: The isomers of the ruthenium−peptide complex. The $[Ru(phen)(bpy')(dppz)]^{2+}$ complex has four isomers; the ruthenium center can be Δ or Λ, and the carboxylate linker can be axial or equatorial to dppz. The HPLC chromatogram at 440 nm (lower left) for the Ru−KYK conjugate shows separation of three main products. The circular dichroism spectra for the three products is presented (lower right).

dichroism spectroscopy (Figure 2). Peaks 1 and 2 give intense CD bands with opposite sign, and they are clearly enantiomers. The circular dichroism spectra confirm that peaks 1 and 2 are Δ and Λ isomers of the ruthenium complex. Peak 3 gives a flat CD spectrum; it is a racemic mixture of the Δ and Λ isomers. As expected, the position of the peptide arm appears to have a greater influence on conjugate mobility than the stereochemistry of the ruthenium metal center. Peaks 1 and 2, eluting near 20 min, appear to be one arm arrangement, and peak 3, eluting near 22 min, appears to be a different arm arrangement. The small peak that elutes before peak 3 was not collected or analyzed; it may be an impurity or perhaps a small amount of separated isomer.

The ability to separate Δ and Λ by HPLC depends on the interactions of the peptide with the ruthenium complex, and the extent of communication between the peptide and ruthenium center varies with peptide composition and with axial or equatorial positioning of the peptide arm. Only the Ru−KYK, Ru−KWK, and Ru−RYR conjugates showed significant splitting of the first peak. Since many of the conjugates did not show any separation of the peak near 20 min, for all of the conjugates only two HPLC fractions were collected and used in experiments. For example, for Ru−KYK, the material from peaks 1 and 2 was combined and is referred to as isomer 1. The material from peak 3 is referred to as isomer 2.

Binding Constants of Ru−Peptide Conjugates. The $[Ru(phen)(bpy')(dppz)]^{2+}$ complex is a DNA "light switch"; it is luminescent only when bound to DNA (*38*). Taking advantage of this property, DNA binding constants were estimated by luminescence titration for several ruthenium−peptide conjugates (Table 2). The $[Ru(phen)_2dppz]^{2+}$ complex binds to DNA with high affinity; the binding constant has been estimated at 10^6-10^7 M^{-1} (*38*, *71*, *72*).

Table 2: Binding Constants of Ruthenium−Peptide Conjugates[a]

conjugate	isomer[b]	K ($\times 10^{-6}$) (M^{-1})	Ru/base pair
Ru−GYA	1	2	0.3
	2	3	0.7
Ru−KAK	1	5 (0.6)	0.4 (0.1)
	2	5	0.6
Ru−KWK	1	1	0.5
	2	5	0.7
Ru−KYK	1	5 (2)	0.3 (0.1)
	2	9	0.7

[a] Binding constants were determined by luminescence titration. A 0.5 μM solution of the Ru−peptide conjugate in 10 mM sodium phosphate (pH 7) and 100 mM NaCl was titrated with CT DNA, and the luminescence intensity was monitored. Binding constants and Ru/base pair values were determined from Scatchard plots. The values were determined in one or two trials. If two trials were performed, the standard deviation is indicated. A binding constant of 3×10^6 M^{-1} was determined for a 0.25 μM solution of $[Ru(phen)_2dppz]^{2+}$. [b] Two isomers of the Ru−peptide conjugate can be separated by HPLC and are numbered according to the order of elution.

For dilute solutions of conjugate (0.5 μM) in 10 mM sodium phosphate and 100 mM NaCl, the binding constants ranged from 1×10^6 to 9×10^6 M^{-1}. Like the untethered metallointercalator, all of our conjugates bind tightly to DNA. The attachment of the short peptide does modulate the binding affinity, but not dramatically. As expected, the Ru−GYA conjugate generally gave the smallest binding constants, and the presence of Lys residues in the tethered peptide increased the DNA binding affinity. There were modest changes in binding affinity as the central position in the lysine peptide was varied, and the binding constants were

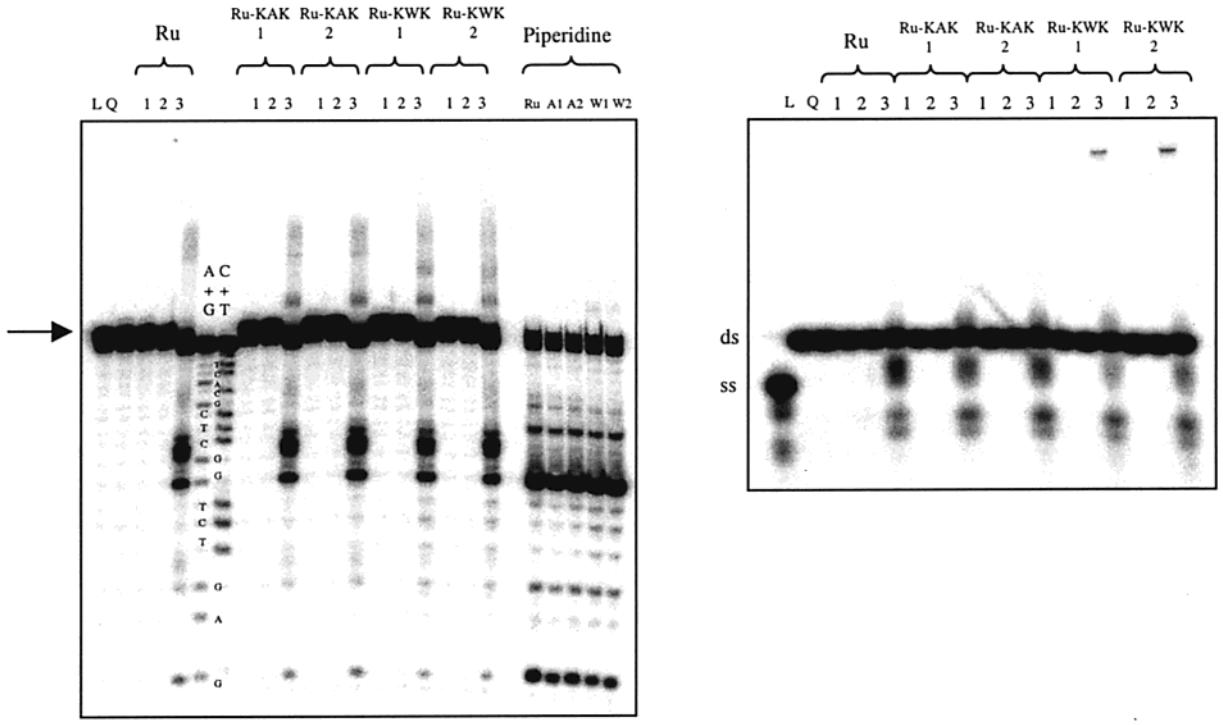

FIGURE 3: Gel analysis of flash−quench cross-linking reactions. The 20-mer duplex (5′-labeled, 5 μM) and $Co(NH_3)_5Cl^{2+}$ quencher (200 μM) were combined with $[Ru(phen)_2dppz]^{2+}$ (Ru), Ru−KAK, or Ru−KWK (10 μM) in a volume of 40 μL. The samples were irradiated for 2 min with the Hg/Xe lamp. After extraction, cross-linking reactions and control samples were analyzed on a 20% denaturing gel (left) and on a 15% native gel (right). Lanes are labeled as follows: A + G, C + T, Maxam−Gilbert sequencing reactions; L, light control, duplex irradiated without quencher or ruthenium; Q, quencher control, duplex irradiated with quencher; 1, dark control, duplex, quencher, and ruthenium combined but not irradiated; 2, duplex and ruthenium irradiated; 3, duplex, quencher, and ruthenium irradiated. On the denaturing gel (left), the parent band is indicated with an arrow. Material above the parent band suggests cross-linking adducts, and material below the parent indicates other reactions at oxidized G. Also, samples of duplex, quencher, and ruthenium were irradiated, treated with piperidine to promote strand scission, and analyzed on the denaturing gel (left).

greatest for the Ru−KYK conjugate. For the Ru−KWK and Ru−KYK conjugates, isomer 2 showed tighter binding than isomer 1. This suggests that the arrangement of the carboxylate arm for isomer 2 produces more favorable interactions of the peptide and DNA.

The number of ruthenium complexes per base pair was also determined from Scatchard plots and ranged from 0.3 to 0.7 (Table 2). Some of these numbers are surprisingly high. Particularly with the pendant 5-mer peptide, we expected no more than one ruthenium complex for every 4−5 base pairs (0.2 Ru/bp). It is possible that the ruthenium−peptide conjugates are clustered on DNA.

Flash−Quench Cross-Linking of Ru−Peptide Conjugates and DNA. We have demonstrated that cross-links can be generated between Ru−peptide conjugates and DNA using flash−quench chemistry. Ru−peptide conjugates were combined with DNA duplex and $[Co(NH_3)_5Cl]^{2+}$ quencher, and the samples were irradiated for several minutes at 442 nm. After phenol−chloroform extraction to remove noncovalent conjugate from the sample, cross-linking adducts were detected by gel electrophoresis or by absorbance measurements.

A typical gel experiment with a 20-mer duplex containing a single GG site and two different Ru−peptide conjugates is presented in Figure 3. As indicated in Scheme 1, the guanine radical can react with the ruthenium−peptide conjugate, but it also can react with oxygen or water to give a variety of permanent guanine lesions. In our experiments we observe a competition between these two pathways. In gel experiments, material above the parent band suggests cross-linking adducts, and material below the parent band indicates reaction with water or oxygen.

With two different peptide conjugates, Ru−KAK and Ru−KWK, a significant amount of material was observed above the parent band on a denaturing polyacrylamide gel (Figure 3, left, lane 3). Light and quencher are both essential ingredients in the cross-linking reaction, and control samples that were kept in the dark (lane 1) or that did not contain quencher (lane 2) showed no signs of cross-linking. The fact that no slow-moving material is observed above the parent band in the dark control samples also rules out a gel shift from the noncovalent ruthenium complex. It appears that the phenol−chloroform extraction effectively removes the noncovalent ruthenium−peptide conjugate from the samples. The ruthenium complex mediates the flash−quench chemistry, and as expected, irradiation of the duplex with light (L) or irradiation of the duplex and quencher (Q) produced essentially no damage to the DNA. Interestingly, a small amount of material was also observed above the parent band for $[Ru(phen)_2dppz]^{2+}$ flash−quench reactions lacking peptide, but clearly the peptide greatly enhances cross-linking and produces a different pattern of bands above the parent strand.

Although oxidative damage or cross-linking to a DNA base does not generally produce DNA strand scission, treatment with hot piperidine can promote cleavage at the damaged site (*53*). Looking below the parent band, significant damage occurs at the 5′ G of the GG site for both $[Ru(phen)_2dppz]^{2+}$

and Ru−peptide reactions (lane 3). Without piperidine treatment, a variety of oxidative products with different gel mobilities are produced; though they arise from damage at the 5′ G, not all of them migrate at the 5′ G.

Upon piperidine treatment, clean strand scission occurs; the material above the parent band disappears, and the fragments observed below the parent band are largely converted into a new product that migrates with the 5′ G. Since our cross-linking adducts are piperidine labile, we can conveniently determine the site of cross-linking. Piperidine treatment reveals that the 5′ G of the GG site is the primary site of oxidative damage. It is the preferred site for reaction with water and oxygen but also for reaction with conjugate. The only significant bands to arise upon treatment with piperidine are the bands at the 5′ G of the GG site and the bands at the 5′ G of a GAG site.

There are some interesting differences between the cross-linking reactions of the Ru−KAK and Ru−KWK conjugates. For Ru−KWK reactions, but not for the Ru−KAK reactions, the smear of slow-moving material extends from the parent band to the wells of the denaturing gel. This difference is more easily visualized on a native gel (Figure 3, right), where only the Ru−KWK lanes show material caught in the wells. However, upon piperidine treatment, the Ru−KAK and Ru−KWK lanes on the denaturing gel are essentially the same (Figure 3, left).

The fraction of DNA that has formed cross-linking adducts can be estimated by integrating the counts above the parent band and dividing by the counts in the entire lane. For this experiment, isomers 1 and 2 of Ru−KAK show 4% and 5% cross-linked DNA, and isomers 1 and 2 of Ru−KWK show 6% and 5% cross-linked DNA. Though they produce a different pattern of slow-moving material on denaturing gels, the two different conjugates give very similar quantitites of cross-linked material. It is important to note that we have not carried out our experiment under single-hit conditions; it is possible that more than one damage event has occurred for each labeled strand. If cleavage of the DNA strand occurs between the cross-linking site and the radiolabel, the adduct will be invisible and the percentages we determine from the gel will underestimate the extent of cross-linking. The pathway that generates guanine lesions through reaction with water or oxygen was favored over peptide cross-linking in this experiment, and in reactions containing ruthenium conjugate and quencher, approximately 30% of the DNA was damaged at the GG site to give guanine oxidation products.

Cross-linking adducts can also be detected through absorbance measurements. Two identical samples of Ru−KYK6 with the quencher and 20-mer duplex were prepared. One was irradiated at 442 nm, and one was kept in the dark. Both samples were extracted to remove the noncovalent ruthenium complex from the sample and then were precipitated by the addition of ethanol. The irradiated sample gave an orange pellet that suggested cross-linking, and the dark control sample gave only a white pellet of DNA. The material was redissolved in 1:1 water−acetonitrile, and absorption spectra were obtained for each sample. The irradiated sample, but not the dark control sample, showed the expected absorbances for the ruthenium complex. By measuring the absorbance at 440 nm of the Ru−KYK6 sample after the irradiation, extraction, and precipitation procedure, the amount of ruthenium conjugate remaining in the sample was found to be 30% of the original amount of the ruthenium conjugate. Again, this number underestimates the extent of cross-linking. We typically use a 20−50 μL sample in irradiation experiments, but this experiment required a 200 μL sample. This large volume will not be irradiated as effectively as a small volume. In addition, after precipitation the orange pellet was not always completely resuspended. The luminescence associated with these samples was also examined (vide infra).

Impact of Peptide Composition on Cross-Linking. To further explore the impact of peptide composition on cross-linking, a family of ruthenium−peptide conjugates was prepared (Table 1). Most of the conjugates contained lysine or arginine residues to promote electrostatic interactions with the negatively charged DNA, but a few conjugates with uncharged Ala-Gly-X-Ala-Gly peptides were also prepared. Although these peptides have lower affinity for DNA, we expected that our ruthenium intercalator would effectively deliver them for cross-linking reaction.

A gel experiment that compares the cross-linking activity of the Ru−KYK conjugate and the Ru−GYA conjugate is pictured in Figure 4. In this experiment, a 40-mer DNA duplex (5 μM) with three GG sites was combined with $[Co(NH_3)_5Cl]^{2+}$ quencher (200 μM) and either $[Ru(phen)_2dppz]^{2+}$, Ru−KYK, or Ru−GYA (20 μM) in a buffer containing sodium phosphate (10 mM, pH 7) and sodium chloride (20 mM). The samples were irradiated at 442 nm for 0, 2, 5, or 15 min (Figure 4, lanes 1−4). Again, material above the parent band suggests cross-linking, and material below the parent suggests reaction of the guanine radical with oxygen or water. There is clearly more cross-linking with Ru−KYK than with Ru−GYA. Nonetheless, the Ru−GYA conjugate does give a significant level of cross-linking and cross-links at higher levels than the ruthenium complex without tethered peptide. In this experiment, the formation of DNA−peptide adducts appears to be the major damage pathway in the presence of Ru−KYK. Prior to piperidine treatment, the levels of damage observed below the parent band are significantly reduced for Ru−KYK samples relative to $[Ru(phen)_2dppz]^{2+}$ samples.

Quantitations of the two gels (Table 3) gives a background level of 4% for the material above the parent band. The lanes for light control, quencher control, $[Ru(phen)_2dppz]^{2+}$, and dark controls all show approximately 4−5% of the lane counts above the parent. The percentage of material above the parent band ranged from 11% to 18% for Ru−KYK and from 7% to 10% for Ru−GYA and did not increase steadily with irradiation time. The data suggest that the reaction is quite efficient and that long irradiation times are not needed. For the Ru−KYK conjugates less than 5% of the DNA reacted with water or oxygen to give lesions at the GG sites, and for the Ru−GYA conjugates 15−20% of the DNA reacted with water or oxygen rather than with peptide.

On piperidine treatment (Figure 4, lane 5), the amount of material above the parent band is reduced, and the damage below the parent band is converted into products that migrate with the 5′ G of the three GG sites. It appears that we are generating cross-linking adducts primarily at the GG sites; the 5′ G is the major damage product revealed by piperidine treatment.

The presence of Lys residues in the peptide has a significant impact on cross-linking, and changing the central

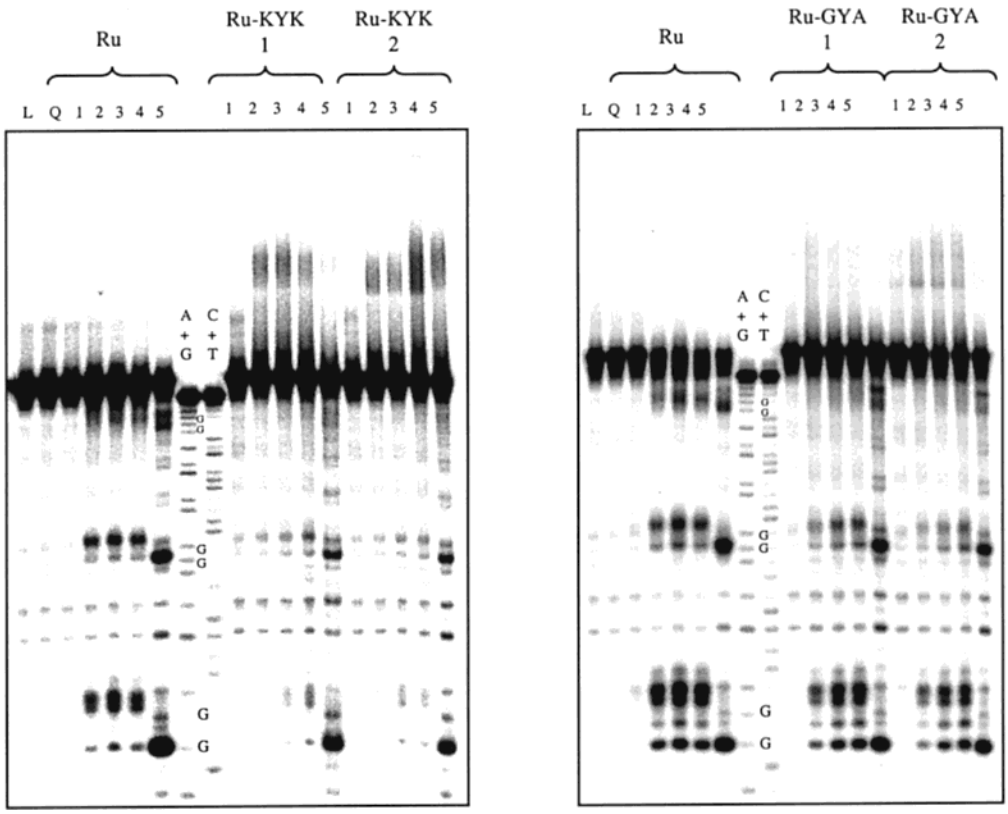

FIGURE 4: Gel analysis of cross-linking with Ru−KYK and Ru−GYA. The 40-mer duplex (5′-labeled, 5 mM) and $[Co(NH_3)_5Cl]^{2+}$ quencher (200 μM) were combined with $[Ru(phen)_2dppz]^{2+}$ (Ru), Ru−KYK, or Ru−GYA (20 μM) in a 20 μL volume. The samples were irradiated for varying amounts of time with the Hg/Xe lamp. After extraction, cross-linking reactions and control samples were analyzed on 15% denaturing gels. Lanes are labeled as follows: A + G, C + T, Maxam−Gilbert sequencing reactions; L, light control; Q, quencher control; 1, dark control; 2−4, duplex, ruthenium, and quencher irradiated for 2, 5, and 15 min; 5, duplex, quencher, and ruthenium irradiated for 15 min and then treated with piperidine.

Table 3: Percentage of Cross-Linked DNA with Ru−KYK and Ru−AYG Conjugates[a]

control reaction[b]	length of irradiation (min)	% cross-linked DNA by gel[c]
L	15	4
Q	15	4
Ru	15	4

conjugate	length of irradiation (min)	% cross-linked DNA by gel[c] isomer 1, isomer 2[d]
Ru−KYK	0	4, 5
	2	15, 11
	5	15, 11
	15	8, 18
Ru−GYA	0	5, 5
	2	8, 9
	5	7, 10
	15	7, 8

[a] Quantitation of the gel presented in Figure 5. [b] L = light control, duplex irradiated. Q = quencher control, duplex and quencher irradiated. Ru = duplex, quencher, and $[Ru(phen)_2dppz]^{2+}$ irradiated. [c] The percentage of cross-linked DNA was estimated by integrating the counts above the parent band and dividing by the counts in the entire lane. [d] Two isomers of the Ru−peptide conjugate can be easily separated by HPLC and are numbered according to the order of elution.

residue in the peptide can produce subtle changes in cross-linking patterns (Ru−KYK vs Ru−KAK). To more systematically explore the impact of peptide composition on cross-linking, a large number of conjugates were compared in a gel experiment and through absorbance measurements. The percentage of cross-linked DNA or cross-linked ruthenium complex was determined for each conjugate and is reported in Table 3. As described previously, both the gel and absorbance methods tend to underestimate the extent of cross-linking, but they do allow for rough comparisons between conjugates.

To measure the amount of cross-linking by absorbance, the 20-mer duplex was combined with the ruthenium complex, and the absorbance at 440 nm was recorded. After addition of quencher, irradiation, extraction, precipitation, and resuspenion, the absorbance at 440 nm was again recorded and was used to calculate the percentage of cross-linked ruthenium conjugate. The data from these experiments (Table 4) suggest higher levels of cross-linking with positively charged peptides containing Lys or Arg and show small changes in the overall levels of cross-linking as the central residue in the peptide is varied. All of the Lys-X-Lys peptides gave 20−36% cross-linked ruthenium complex, and the Gly-X-Ala peptides gave 5% and 15%. The Ru−GAA conjugate showed essentially no cross-linking; only 5% of the 440 nm signal was retained after irradiation and extraction. Introducing a single lysine or tyrosine residue increased the extent of cross-linking to 15%. Among the Lys-X-Lys conjugates, the order of increasing cross-linking for this experiment was Ru−KEK < Ru−KAK ∼ Ru−KSK < Ru−KHK < Ru−KWK ∼ Ru−KYK ∼ Ru−KKK. Changing the length of the peptide from a 5-mer to a 6-mer had little impact on the level of cross-linking; the Ru−KYK and Ru−KYK6 conjugates gave very similar percentages in this

Table 4: Percentage of Cross-Linking Product for Ru−Peptide Conjugates

control reaction	% cross-linked Ru by absorbance[a]	% cross-linked DNA by gel[b]
L		1
Ru	6	9
Q Ru−KWK 1		2
D Ru−KYK 1	<1	
Q Ru−KYK 1	<1	

conjugate	% cross-linked Ru by absorbance[a] isomer 1, isomer 2[c]	% cross-linked DNA by gel[b] isomer 1, isomer 2
Ru−GAA	6, 5	
Ru−GKA	15, 14	
Ru−GYA	14, 10	
Ru−KAK	26, 19	33, 32
Ru−KEK	23, 20	31, 25
Ru−KHK	31, 29	40, 38
Ru−KKK	36, 34	37, 37
Ru−KSK	29, 22	30, 31
Ru−KWK	34, 34	37, 39
Ru−KYK	36, 32	30, 41
Ru−KYK6	39, 31	
Ru−RYR	21, 22	

[a] The percentage of cross-linked ruthenium complex was determined by measuring the absorbance at 440 nm of a sample before and after irradiation, extraction, and precipitation. [b] The percentage of cross-linked DNA was estimated by quantitating the counts above the parent band and dividing by the counts in the entire lane. [c] Two isomers of the Ru−peptide conjugate can be easily separated by HPLC and are numbered according to the order of elution.

absorbance experiment and also in gel experiments. Though previous gel experiments suggested that conjugates with Arg and Lys were comparable, this absorbance experiment showed reduced cross-linking with Ru−RYR relative to Ru−KYK. The differences in cross-linking between the two isomers were small, and for all the conjugates except Ru−KWK and Ru−RYR, the percentage of cross-linking was slightly higher for isomer 1.

A gel experiment with a 40-mer DNA substrate gave very similar data (Table 4). The percentage of cross-linked DNA ranged from 25% to 40%. Varying the central residue had a modest effect on cross-linking; the order of increasing cross-linking was Ru−KEK < Ru−KSK ∼ Ru−KAK < Ru−KKK < Ru−KYK < Ru−KWK < Ru−KHK. Again, the differences in cross-linking between the two isomers were fairly small.

Role of Ruthenium−Metallointercalator in Flash−Quench Cross-Linking Reactions. In our cross-linking system the ruthenium intercalator was expected to play two important roles: (i) to initiate cross-linking through oxidation of DNA or peptide and (ii) to provide DNA binding affinity for small peptides. Clearly, the ruthenium intercalator does initiate cross-linking through the flash−quench cycle. Control samples lacking the ruthenium complex or quencher showed no cross-linking. To examine whether the ruthenium complex also was required for the delivery of peptides to DNA, we completed experiments with untethered peptide. A typical experiment is presented in Figure 5.

We prepared two sets of cross-linking reactions with the 20-mer duplex and cobalt quencher. One set contained a ruthenium−peptide conjugate, and one set contained equal concentrations of untethered peptide and $[Ru(phen)_2dppz]^{2+}$. The samples were irradiated, extracted, and analyzed by gel

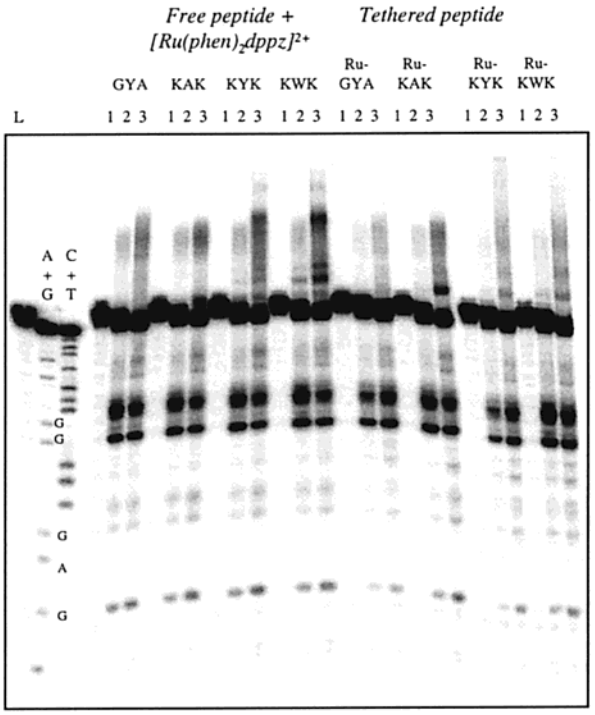

FIGURE 5: Gel analysis of cross-linking with untethered and tethered peptides. The 20-mer duplex (5′-labeled, 5 μM) and $[Co(NH_3)_5Cl]^{2+}$ quencher (200 μM) were combined with $[Ru(phen)_2dppz]^{2+}$ and free peptide or with isomer 2 of a ruthenium−peptide conjugate. The samples were irradiated for 1 min with the He/Cd laser. After extraction, the cross-linking and control samples were analyzed on a 20% denaturing gel. Lanes are labeled as follows: A + G, C + T, Maxam−Gilbert sequencing reactions; L, light control; 1, dark control; 2, duplex, quencher, and either $[Ru(phen)_2dppz]^{2+}$ (2 μM) and free peptide (2 μM) or the ruthenium−peptide conjugate (2 μM); 3, duplex, quencher, and either $[Ru(phen)_2dppz]^{2+}$ (20 μM) and free peptide (20 μM) or the ruthenium−peptide conjugate (20 μM).

electrophoresis. As earlier, cross-linking was assessed through measurements of the increase in intensity of the slowly migrating band in the gel. Interestingly, we observed greater levels of cross-linking with the free peptides than with the tethered peptides at both 2 and 20 μM concentrations (Figure 5, lanes 2 and 3). Clearly, the metallointercalator is not required for peptide delivery. Even for the uncharged GYA peptide, the peptide that is expected to have the lowest affinity for DNA, the cross-linking is greater with free peptide. As observed in all gel experiments, the peptides containing Trp and Tyr gave a distinctive pattern of bands above the parent band and created a slow mobility smear that extended right to the wells. This was observed both with tethered and free peptides containing Trp and Tyr.

Characterization of Cross-Linked Material by Spectroscopy. As is evident in Figure 6, cross-linking of the Ru−peptide conjugate versus the free peptide is advantageous, nonetheless, in that this cross-linking leads to the incorporation of a luminescent tag. To examine this luminescence labeling, two identical samples of the Ru−KYK6 conjugate with quencher and 20-mer duplex were prepared. One was irradiated at 442 nm, and one was kept in the dark. Both samples were extracted to remove the noncovalent ruthenium complex from the sample and then were precipitated by the addition of ethanol. The material was redissolved in 1:1 water−acetonitrile, and absorbance and luminescence spectra were obtained for each sample (Figure 6). The irradiated

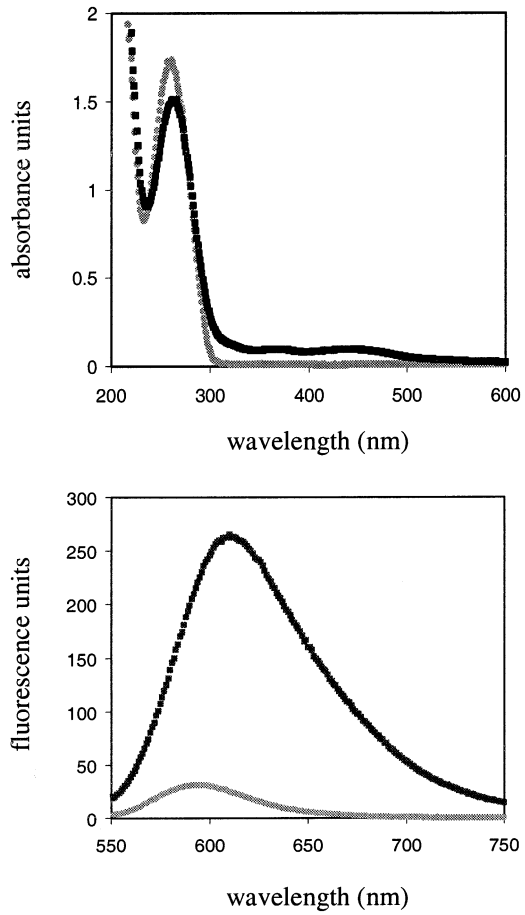

FIGURE 6: Absorbance and luminescence spectra for cross-linked material. Two samples of the 20-mer duplex, Ru−KYK6, and quencher were prepared, and one sample was irradiated. The absorbance (top) and luminescence (bottom) spectra for the irradiated (black squares) and dark control (gray circles) samples are shown. To obtain a fluorescence spectrum, the samples were excited at 442 nm.

sample, but not the dark control sample, showed the expected absorbances for the ruthenium complex in the visible region and, with excitation at 442 nm, gave an emission peak centered around 610 nm.

Characterization of Cross-Linked Material by Mass Spectrometry. Cross-linked and dark control samples were also submitted for MALDI mass spectrometry analysis, and the molecular ion patterns and intensities in these samples were compared. The masses expected for the two intact DNA strands (m/z = 6069 and 6167) were observed in the dark control samples, but in the irradiated samples the peak corresponding to the strand with the GG site was greatly reduced. Clearly, this strand is being converted into other products. Besides observing the loss of this parent DNA band, analysis of a cross-linking sample containing Ru−KAK revealed new peaks (m/z = 7346 and 8626) that roughly match the expected mass for one and two Ru−KAK conjugates cross-linked to the GG strand. Peptide−DNA conjugates are well-known to have poor desorption characteristics (*70*), and such was the case for these samples, limiting high-resolution characterization and comparisons.

DISCUSSION

Metallointercalator−Peptide Conjugates as a Model System for Studying DNA−Protein Cross-Linking. To study DNA−protein cross-linking, we have tethered short peptides to a ruthenium intercalator. The ruthenium intercalator, $[Ru(phen)(bpy')(dppz)]^{2+}$, binds with high affinity to DNA and initiates cross-linking through a flash−quench reaction (Scheme 1). The peptide provides a variety of functional groups that can react with oxidized DNA to forge cross-links. In the flash−quench reaction, the Ru(III) complex, a powerful oxidant, is generated in situ by irradiating a sample of the Ru−peptide conjugate, oxidative quencher, and DNA with visible light. The Ru(III) complex oxidizes guanine, the base with the lowest oxidation potential. In turn, the guanine radical reacts with water, oxygen, or the tethered peptide to generate permanent DNA damage, either oxidized guanine products or DNA−peptide cross-links.

Evidence for the formation of DNA−peptide cross-links was provided by gel analysis and by absorbance measurements. A sample containing the Ru−peptide conjugate, DNA duplex, and $[Co(NH_3)_5Cl]^{2+}$ quencher was irradiated at 442 nm and then extracted to remove any unlinked Ru−peptide conjugate. For irradiated samples, but not for dark control samples, material that migrates more slowly than the full-length DNA strand was detected on denaturing and native polyacrylamide gels, and the absorbance and fluorescence characteristics expected for the Ru−peptide conjugate were observed. The cross-linking reaction is very efficient; indeed, 30−40% of the DNA substrate or ruthenium complex can be cross-linked during a 1 or 2 min irradiation. The ratio of oxidized guanine product to DNA−peptide cross-link varied with peptide composition, but generally the reaction with water or oxygen was favored over the reaction with peptide.

Our strategy for DNA−peptide cross-linking is fairly simple. We are able to control important variables and examine cross-linking levels. By systematically mutating the tethered peptide, we have determined the impact of peptide composition on binding and cross-linking. Through experiments with tethered and untethered peptide, we have also probed the importance of the metallointercalator for delivery of the peptides to DNA.

The Tethered Peptide. Our solid-phase method for preparing ruthenium−peptide conjugates is a general one and is compatible with a variety of peptide compositions. Only peptides containing cysteine proved troublesome. Apart from studies of DNA−peptide cross-linking, there are a variety of reasons for incorporating a ruthenium metal center into a peptide (*73*), and we have established a route to some very interesting chimeras.

For binding and cross-linking studies we attached 5-mer peptides to our ruthenium complexes. These peptides should be long enough to allow interactions between the peptide and DNA, even when the dppz ligand is intercalated into the base stack, and short enough to remain unstructured. The N-terminal Ala was intended as a flexible spacer, the C-terminal Gly simplified synthesis and was intended to adsorb end effects, and the three central residues were varied. Though we did not thoroughly explore the impact of peptide length on binding or cross-linking, we did compare the cross-linking levels of a 5-mer and 6-mer peptide but observed very little difference.

In our studies, we have considered two types of peptides: peptides with positively charged residues (Lys or Arg) at positions 2 and 4 and peptides with aliphatic residues (Ala and Gly) at positions 2 and 4. Peptides containing lysine

and arginine can have favorable electrostatic interactions with the polyanionic backbone of DNA. Also, lysine can serve as a nucleophile to attack oxidized guanine sites. Using a model system, Morin and Cadet have demonstrated that amino or hydroxy nucleophiles form cross-links with oxidized 2′-deoxyguanine (*26*−*28*). In contrast, Ala and Gly are bystanders; they are not expected to contribute to binding, and they are not expected to be as reactive as lysine or arginine. By creating peptides with Ala and Gly, we focused attention on the reactivity of position 3 of the peptide.

The peptide composition does impact binding and cross-linking. Through luminescence titration we determined that the conjugates bearing lysine residues generally showed greater affinity for DNA than the Ru−GYA conjugate; the additional positive charge of these conjugates increases DNA binding. The binding constants for Lys-X-Lys conjugates ranged from 1×10^6 to 9×10^6 M^{-1}, and the binding constants for the two isomers of the Ru−GYA conjugate were 2×10^6 and 3×10^6 M^{-1}. These differences in binding affinity are not large, and under the conditions of our cross-linking experiments, high DNA concentrations and lower salt, there will not be significant differences in the percentage of bound conjugate as the peptide composition of the conjugate is varied.

The Lys-X-Lys or Arg-X-Arg peptides gave the highest levels of cross-linking. In a gel experiment the percentage of cross-linked DNA was approximately two times greater for Ru−KYK than for Ru−GYA. This difference in cross-linking activity may be attributed to increased interaction between the DNA and the positively charged peptide or to the reactivity of the Lys residues. As demonstrated with model systems and in studies with MutY, lysine can attack oxidized guanine to form cross-links (*14*, *26*−*28*).

The central residue in the 5-mer peptide was tuned to explore the reactivity of individual amino acids. At position 3 we tested seven different amino acids: Ala, Glu, His, Lys, Ser, Trp, and Tyr. These seven residues provide a variety of functional groups. We expected that incorporation of Ala at the central position would give the least reactive conjugate. With Glu and His we introduce a negatively charged acid group and an imidazole group. From the results of Morin and Cadet we expected Lys and Ser to act as nucleophiles and to attack at the guanine radical (*26*−*28*). The Trp and Tyr peptides are particularly interesting because these aromatic residues can intercalate into DNA and can be oxidized. Previously, in flash−quench experiments with the ruthenium complex and tripeptides, both the Trp and Tyr radicals were observed by transient absorption spectroscopy (*56*, *57*). The guanine radical can oxidize Trp and Tyr if they are intercalated into the DNA π stack; therefore, a different cross-linking mechanism, a mechanism that involves a peptide radical, is possible with these two residues.

Variation of the central residue did produce some change in binding affinity. The binding constants increased in the order Ru−KWK < Ru−KAK < Ru−KYK. This order is not the order expected for the free peptide. The Trp residue, through intercalation, is expected to contribute binding affinity. By tethering the peptides to an intercalating moiety, we constrain them, and perhaps the tethered Trp peptide is not ideally positioned for intercalation into the base stack.

The differences observed in cross-linking were actually quite small as the central position in the peptide was varied; the overall levels of cross-linking were very similar for all of the Lys-Lys conjugates. Slightly lower percentages of cross-linked ruthenium were estimated for the Ala, Glu, and Ser conjugates by absorbance measurements. Though the levels of cross-linking with Trp and Tyr were not higher, we did consistently observe a different pattern of slow-moving products with conjugates containing these residues. Perhaps this is due to different mobility properties of these peptide adducts, but it might also reflect a peptide radical mechanism and a different set of products. On piperidine treatment, the damage pattern observed for Trp and Tyr conjugates is very similar to the pattern observed with all the other conjugates. Even if a Trp or Tyr radical is generated in our flash−quench reactions, we still see permanent lesions primarily at the 5′ G of the GG site. It has been previously suggested that Tyr preferentially cross-links at thymine bases (*12*, *74*), but we do not see evidence of significant thymine cross-linking in our experiments.

The Ruthenium Metallointercalator. The ruthenium metallointercalator was originally expected to perform three important functions: (i) to produce guanine radical and initiate cross-linking upon irradiation, (ii) to deliver low-affinity peptides to DNA, and (iii) to provide a luminescent tag for the conjugates and cross-linking adducts.

Clearly, $[Ru(phen)(bpy')(dppz)]^{2+}$ does perform the first function. Without the ruthenium complex, quencher, or irradiation there is no cross-linking between DNA and peptide. But must the peptides be harnessed to the ruthenium intercalator in order to achieve efficient cross-linking? To explore the importance of this second function, we compared the cross-linking of untethered and tethered peptides. In these experiments, $[Ru(phen)_2dppz]^{2+}$ was included with the untethered peptide to initiate the oxidation of guanine.

Our results clearly demonstrate that the peptide does not need to be tethered; greater levels of cross-linking were actually achieved with free peptide than with the corresponding ruthenium−peptide conjugates. By harnessing peptides to the ruthenium intercalator, we increase their affinity for DNA by 2 orders of magnitude and increase the local concentration of peptide near the DNA duplex. For peptides that do not contain intercalating residues, and especially for the conjugates containing glycine and alanine at positions 2 and 4, the increase in affinity is expected to be greatest. Since we observe cross-linking with the untethered G-X-A peptides, it appears that even peptides that are transiently associated with DNA can be efficiently cross-linked.

It is important to note that the $[Ru(phen)_2dppz]^{2+}$ complex has a longer lifetime and a higher oxidation potential than the $[Ru(phen)(bpy')(dppz)]^{2+}$ complex (*45*, *56*, *57*, *75*); thus the $[Ru(phen)_2dppz]^{2+}$ complex should oxidize guanine more efficiently. The greater cross-linking observed with free peptide might be partly explained by the use of $[Ru(phen)_2dppz]^{2+}$ rather than $[Ru(phen)(bpy')(dppz)]^{2+}$ in the reactions. Yet, the amount of guanine oxidation product did not differ significantly for reactions with free peptide and $[Ru(phen)_2dppz]^{2+}$ and reactions with $[Ru(phen)(bpy')(dppz)]^{2+}$ conjugates. It is also likely that the tethered peptides are constrained and not able to achieve intimate interactions with the DNA. The two separated isomers of the Ru−peptide conjugate provide different orientations of the peptide arm, but neither isomer appears to be perfectly suited for peptide delivery and cross-linking. Isomer 2 generally gave higher

binding constants (Table 2) but did not always give higher levels of cross-linking.

Though it may reduce the extent of cross-linking, there are still important reasons for attaching peptides to the ruthenium intercalator. The rich spectroscopic properties of the ruthenium complex provide a convenient absorbance assay that allows for quantitation of cross-linking, and through luminescence titration, the binding constants of ruthenium−peptide conjugates can be directly determined. More importantly, we have demonstrated that the cross-linking adducts generated by the flash−quench technique are luminescent. Thus we have created a photoactivated probe for DNA−peptide cross-linking; each cross-linking event attaches a luminescent tag to the DNA.

Insights and Applications for DNA−Protein Cross-Linking. Our studies with Ru−peptide conjugates have provided some valuable insights into cross-linking chemistry. We have demonstrated that the reaction between oxidized DNA and peptides is very efficient and requires only transient interaction between the DNA and peptide. Although positively charged residues certainly facilitate cross-linking, we have shown that peptides of diverse composition can form oxidative cross-links with DNA.

We have demonstrated a new strategy for generating DNA−peptide adducts at a single GG site in a DNA duplex, and this may provide a useful tool for the study of DNA−protein repair mechanisms (*3*). We can now consider targeting cross-linking still more specifically through the site specificity of the pendant peptide. In addition, we are particularly interested in probing the biological relevance of DNA charge transport, and this study suggests a strategy for identifying proteins that participate in electron transfer with DNA. By exploiting the flash−quench cross-linking chemistry and the luminescence of a DNA−tethered ruthenium complex, it may actually be possible to extract such proteins from cellular lysates.

CONCLUSION

Through the flash−quench chemistry of a ruthenium intercalator, a collection of ruthenium−peptide conjugates and free peptides have been efficiently cross-linked to DNA. The composition of the peptide affects both the DNA binding affinity and the cross-linking efficiency of ruthenium−peptide conjugates. By attaching peptides to the ruthenium complex, we have created a photoactivated luminescent cross-linking reagent.

ACKNOWLEDGMENT

We are grateful to the Biopolymer Synthesis Facility at Caltech for the preparation of peptides, to Dr. Mona Shagoli for MALDI analysis of the cross-linking adducts, and to Dr. Hans-Achim Wagenknecht for synthesis of the ruthenium complex.

REFERENCES

1. Kelly, S. O., and Barton, J. K. (1999) *Metal Ions Biol. 36*, 211.
2. Wiseman, H., and Halliwell, B. (1996) *Biochem. J. 313*, 17−29.
3. Ames, B. N., Shigenaga, M. K., and Hagen, T. M. (1993) *Proc. Natl. Acad. Sci. U.S.A. 90*, 7915−7922.
4. Marnett, L. J., and Burcham, P. C. (1993) *Chem. Res. Toxicol. 6*, 771−785.
5. Minko, I. G., Zou, Y., and Lloyd, R. S. (2002) *Proc. Natl. Acad. Sci. U.S.A. 99*, 1905−1909.
6. Nguyen, K. L., Steryo, M., Kurbanyan, K., Nowitzki, K. M., Butterfield, S. M., Ward, S. R., and Stemp, E. D. A. (2000) *J. Am. Chem. Soc. 122*, 3585−3594.
7. Costa, M. (1990) *J. Cell. Biochem. 44*, 127.
8. Izzotti, A., Cartiglia, C., Taningher, M., De Flora, S., and Balansky, R. (1999) *Mutat. Res. 446*, 215−223.
9. Quievryn, G., and Zhitkovich, A. (2000) *Carcinogenesis 21*, 1573−1580.
10. Chakrabarti, S. K., Bai, C., and Subramanian, K. S. (2001) *Toxicol. Appl. Pharmacol. 170*, 153−165.
11. Izzoti, A., Bagnasco, M., Camoirano, A., Orlando, M., and De Flora, S. (1998) *Mutat. Res. 400*, 233−244.
12. Altman, S. A., Zastawny, T. H., Randers-Eichhorn, L., Cacciuttolo, M. A., Akman, S. A., Dizdaroglu, M., and Rao, G. (1995) *Free Radical Biol. Med. 19*, 897.
13. Gavin, I. M., Melnick, S. M., Yurina, N. P., Khabarova, M. I., and Bavykin, S. G. (1998) *Anal. Biochem. 263*, 26.
14. Hickerson, R. P., Chepanoske, C. L., Williams, S. D., David, S. S., and Burrows, C. J. (1999) *J. Am. Chem. Soc. 121*, 9901−9902.
15. Pinto, A. J., and Lippard, S. J. (1985) *Biochim. Biophys. Acta 780*, 167−180.
16. Hashimoto, M., Greenberg, M. M., Kow, Y. W., Hwang, J.-T., and Cunningham, R. P. (2001) *J. Am. Chem. Soc. 123*, 3161−3162.
17. Voitkun, V., and Zhitkovich, A. (1999) *Mutat. Res. 424*, 97−106.
18. Shaham, J., Bomstein, Y., Meltzer, A., Kaufman, Z., Palma, E., and Ribak, J. (1996) *Carcinogenesis 17*, 121.
19. Conaway, C. C., Whysner, J., Verna, L. K., and Williams, G. M. (1996) *Pharmacol. Ther. 71*, 29−55.
20. Saito, I., and Matsura, T. (1995) *Acc. Chem. Res. 18*, 134−141.
21. Shetlar, M. D. (1980) *Photochem. Photobiol. Rev. 5*, 105−197.
22. Strniste, G. F., and Rall, S. C. (1976) *Biochemistry 15*, 1712.
23. Blazek, E. R., and Hariharan, P. V. (1984) *Photochem. Photobiol. 40*, 5.
24. Ramakrishnan, N., Clay, M. E., Xue, L., Evans, H. H., Rodriguez-Antunez, A., and Oleinick, N. L. (1988) *Photochem. Photobiol. 48*, 297.
25. Villanueva, A., Canete, M., Trigueros, C., Rodriguez-Borlado, L., and Juarranz, A. (1993) *Biopolymers 33*, 239.
26. Morin, B., and Cadet, J. (1995) *J. Am. Chem. Soc. 117*, 12408−12415.
27. Morin, B., and Cadet, J. (1995) *Chem. Res. Toxicol. 8*, 792−799.
28. Morin, B., and Cadet, J. (1994) *Photochem. Photobiol. 60*, 102−109.
29. Erkkila, K. E., Odom, D. T., and Barton, J. K. (1999) *Chem. Rev. 99*, 2777.
30. Kielkopf, C. L., Erkkila, K. E., Hudson, B. P., Barton, J. K., and Rees, D. C. (2000) *Nat. Struct. Biol. 7*, 117−121.
31. Johann, T. W., and Barton, J. K. (1996) *Philos. Trans. R. Soc. London, Ser. A 354*, 299−324.
32. Núñez, M. E., and Barton, J. K. (2000) *Curr. Opin. Chem. Biol. 4*, 199−206.
33. Sardesai, N. Y., Zimmermann, K., and Barton, J. K. (1994) *J. Am. Chem. Soc. 116*, 7502−7508.
34. Fitzsimons, M. P., and Barton, J. K. (1997) *J. Am. Chem. Soc. 119*, 3379−3380.
35. Copeland, K. D., Fitzsimons, M. P., Houser, R. P., and Barton, J. K. (2002) *Biochemistry 41*, 343−356.
36. Sissi, C., Rossi, P., Felluga, F., Formaggio, F., Palumbo, M., Tecilla, P., Toniolo, C., and Scrimin, P. (2001) *J. Am. Chem. Soc. 123*, 3169−3170.
37. Tabor, A. B. (1996) *Tetrahedron 52*, 2229−2234.
38. Friedman, A. E., Chambron, J.-C., Sauvage, J.-P., Turro, N. J., and Barton, J. K. (1990) *J. Am. Chem. Soc. 112*, 4960−4962.
39. Hartshorn, R. M., and Barton, J. K. (1992) *J. Am. Chem. Soc. 114*, 5919−5925.
40. Olson, E. J. C., Hu, D., Hörmann, A., Jonkman, A. M., Arkin, M. R., Stemp, E. D. A., Barton, J. K., and Barbara, P. F. (1997) *J. Am. Chem. Soc. 119*, 11458−11467.
41. Murphy, C. J., Arkin, M. R., Jenkins, Y., Ghatlia, N. J., Bossmann, S. H., Turro, N. J., and Barton, J. K. (1993) *Science 262*, 1025−1029.
42. Arkin, M. R., Stemp, E. D. A., Pulver, S. C., and Barton, J. K. (1997) *Chem. Biol. 4*, 389−400.

43. Chang, I. J., Gray, H. B., and Winkler, J. R. (1991) *J. Am. Chem. Soc. 113*, 7056.
44. Dunn, D. A., Lin, V. H., and Kochevar, I. E. (1992) *Biochemistry 31*, 11620.
45. Stemp, E. D. A., Arkin, M. R., and Barton, J. K. (1997) *J. Am. Chem. Soc. 119*, 2921.
46. Steenken, S., and Jovanovic, S. V. (1997) *J. Am. Chem. Soc. 119*, 617.
47. Sugiyama, H., and Saito, I. (1996) *J. Am. Chem. Soc. 118*, 7063−7068.
48. Prat, F., Houk, K. N., and Foote, C. S. (1998) *J. Am. Chem. Soc. 120*, 845−846.
49. Nakatani, K., Dohno, C., and Saito, I. (1999) *J. Am. Chem. Soc. 121*, 10854−10855.
50. Núñez, M. E., Hall, D. B., and Barton, J. K. (1999) *Chem. Biol. 6*, 85.
51. Schuster, G. B. (2000) *Acc. Chem. Res. 33*, 253−260.
52. Giese, B. (2000) *Acc. Chem. Res. 33*, 631−636.
53. Burrows, C. J., and Muller, J. G. (1998) *Chem. Rev. 98*, 1109−1151.
54. Luo, W., Muller, J., Rachlin, E. M., and Burrows, C. J. (2000) *Org. Lett. 2*, 613−616.
55. Cadet, J., Berger, M., Buchko, G. W., Joshi, P. C., Raoul, S., Ravanat, J.-L. (1994) *J. Am. Chem. Soc. 116*, 7403−7404.
56. Wagenknecht, H.-A., Stemp, E. D. A., and Barton, J. K. (2000) *J. Am. Chem. Soc. 122*, 1−7.
57. Wagenknecht, H.-A., Stemp, E. D. A., and Barton, J. K. (2000) *Biochemistry 39*, 5483−5491.
58. Rajeswari, M. R., Montenay-Garestier, T., and Helene, C. (1987) *Biochemistry 26*, 6825−6831.
59. Rajeswari, M. R. (1996) *J. Biomol. Struct. Dyn. 14*, 25.
60. Dickeson, J. E., and Summers, L. A. (1970) *Aust. J. Chem. 23*, 1023.
61. Ciana, L. D., Hamachi, I., and Meyer, T. J. (1989) *J. Org. Chem. 54*, 1731−1735.
62. Gillard, R. D., Osborn, J. A., and Wilkinson, G. J. (1965) *J. Chem. Soc.*, 1951−1965.
63. Amouyal, E., Hornsi, A., Chambron, J. C., and Sauvage, J. P. (1990) *J. Chem. Soc., Dalton Trans. 6*, 1841.
64. Strouse, G. F., Anderson, P. A., Schoonover, J. R., Meyer, T. J., and Keene, F. R. (1992) *Inorg. Chem. 31*, 3004−3006.
65. Anderson, P. A., Deacon, G. B., Haarmann, K. H., Keene, R., Meyer, T. J., Reitsma, D. A., Skelton, B. W., Strouse, G. F., Thomas, N. C., Treadway, J. A., and White, A. H. (1995) *Inorg. Chem. 34*, 6145−6157.
66. Gill, S. C., and von Hipple, P. H. (1989) *Anal. Biochem. 182*, 319−326.
67. Scatchard, G. (1949) *Ann. N.Y. Acad. Sci. 51*, 660−672.
68. Klotz, I. M. (1997) *Ligand−Receptor Energetics*, John Wiley & Sons, New York.
69. Maniatis, T., and Fritsch, E. F. (1982) *Molecular Cloning*, Cold Spring Harbor Laboratory, Plainview, NY.
70. Jensen, O. N., Kulkarni, S., Aldrich, J. V., and Barofsky, D. F. (1996) *Nucleic Acids Res. 24*, 3866−3872.
71. Haq, I., Lincoln, P., Suh, D., Nordén, B., Chowdry, B. Z., and Chaires, J. B. (1995) *J. Am. Chem. Soc. 117*, 4788−4796.
72. Lincoln, P., Broo, A., and Nordén, B. (1996) *J. Am. Chem. Soc. 118*, 2644−2653.
73. Kise, K. J., and Bowler, B. E. (2002) *Inorg. Chem. 41*, 379−386.
74. Nackerdien, Z., Rao, G., Cacciuttolo, M. A., Gajewski, E., and Dizdaroglu, M. (1991) *Biochemistry 30*, 4873−4879.
75. Juris, A., Balzani, V., Barigelletti, F., Campagna, S., Belser, P., and Van Zelewsky, A. (1988) *Coord. Chem. Rev. 84*, 85−277.

BI020407B